IJST (2013) 37A4: 513-526
Iranian Journal of Science & Technology

http://ijsts.shirazu.ac.ir

A new algorithm for solving one-dimensional Schrödinger equations in the reproducing kernel space

M. Mohammadi and R. Mokhtari*

Department of Mathematical Sciences, Isfahan University of Technology, Isfahan 84156-83111, Iran
E-mail: mokhtari@cc.iut.ac.ir & m_mohammadi@math.iut.ac.ir

Abstract

On the basis of a reproducing kernel space, an iterative algorithm for solving the one-dimensional linear and nonlinear Schrödinger equations is presented. The analytical solution is shown in a series form in the reproducing kernel space and the approximate solution is constructed by truncating the series. The convergence of the approximate solution to the analytical solution is also proved. The method is examined for the single soliton solution and interaction of two solitons. Numerical experiments show that the proposed method is of satisfactory accuracy and preserves the conservation laws of charge and energy. The numerical results are compared with both the analytical and numerical solutions of some earlier papers in the literature.

Keywords: Schrödinger equations; reproducing kernel space

1. Introduction

Finding analytical and numerical solutions of various types of partial differential equations (PDEs) is a very important and attractive subject in the study of many physical and engineering model problems [1-10]. One of the most important equations of mathematical physics is the nonlinear Schrödinger equation (NLSE) with several applications in many different fields such as plasma physics, nonlinear optics, water waves, and bimolecular dynamics [11-14]. Its importance comes from two of the most basic processes in a physical system, namely dispersion and nonlinearity. The solutions of the NLSE are balanced due to competing forces of nonlinearity and dispersion. The typical example of such a balanced solution is soliton. It can be solved analytically by using the inverse scattering transform for limited initial conditions [15-17]. Moreover, in real physical systems, existence of driving forces or dissipation may give rise to additional perturbations to the model and, hence, makes it analytically intractable. In order to understand the dynamics of the complicated perturbed soliton models, one has to use numerical simulations. There have been numerous investigations on numerical solutions of variants of the NLSE based on the finite difference [18-25], finite element [26, 27, 28], discontinuous Galerkin [29, 30], differential quadrature [31, 32], radial basis functions collocation [33] and spectral [34, 35] methods. Hu et al. developed a grid method for numerically solving the n-dimensional bound-state Schrödinger equation based on the reproducing kernel Hilbert space and radial basis approximation theory [36]. Recently, Dereli used a meshless kernel-based method of lines for the numerical solution of nonlinear Schrödinger equation [37].

The theory of reproducing kernels [38], was used for the first time at the beginning of the 20th century by S. Zaremba in his work on boundary value problems for harmonic and biharmonic functions. This theory has been successfully applied for solving numerous problems, see e.g. [39-41] and references cited therein.

In this study, an iterative method for solving the nonlinear Schrödinger equation in the reproducing kernel space is proposed. We decompose the nonlinear Schrödinger equation to a coupled system of nonlinear partial differential equations which is solved by using the reproducing kernel method. The advantages of the approach must lie in the following facts. The approximate solution converges uniformly to the analytical solution. The method is mesh free, easily implemented and capable of treating the various boundary conditions. Since the method needs no time discretization, the time in which the approximate solution is computed, from the both elapsed time and stability problem point of views, is not important. Also, we can evaluate the approximate solution $u_{n,m}(x,t)$ for fixed n and m once, and use it over and over. Like

*Corresponding author
Received: 4 October 2012 / Accepted: 18 May 2013

in [42], we work with the reproducing kernel spaces and basis functions for the vector-valued functions, but we avoid having to practise the Gram-Schmidt orthogonalization process. Therefore, required computational time can be somewhat saved.

The rest of the paper is organized as follows. In section 2 the governing equation is described. Several reproducing kernel spaces are defined in section 3. The method implementation and convergence analysis are given in section 4. Numerical results are presented in section 5. The last section is a brief conclusion.

2. Governing equation

Consider the initial-value problem for the one-dimensional NLSE

$$\begin{cases} i\,\dfrac{\partial u}{\partial t}+\eta\dfrac{\partial^2 u}{\partial x^2}+q|u|^p u=0, \quad (x,t)\in(-\infty,\infty)\times(0,T) \\ u(x,0)=\phi(x), \end{cases}$$

where $i=\sqrt{-1}$, $\eta\neq 0$, $q\geq 0$ and $p>0$ are real constants, and $u(x,t)$ which governs weakly nonlinear, strongly dispersive and almost monochromatic wave, is a complex-valued function of the spatial coordinate x and time t. In order to compute a numerical solution on the interval $[a,b]$, artificial boundary conditions $u(a,t)=u(b,t)=0$ is chosen to model the physical conditions that $u\to 0$ as $x\to\pm\infty$. Let

$$u(x,t)=u_1(x,t)+i\,u_2(x,t),$$
$$\phi(x)=\phi_1(x)+i\,\phi_2(x).$$

After homogenizing the initial condition, we get the following system of partial differential equations

$$\begin{cases} \dfrac{\partial^2 u_1}{\partial x^2}-\dfrac{1}{\eta}\dfrac{\partial u_2}{\partial t}=-\dfrac{\partial^2\phi_1}{\partial x^2}-\dfrac{q}{\eta}(u_1+\phi_1)\left((u_1+\phi_1)^2+(u_2+\phi_2)^2\right)^{\frac{p}{2}}, \quad (x,t)\in\Omega=(a,b)\times(0,T) \\ \dfrac{1}{\eta}\dfrac{\partial u_1}{\partial t}+\dfrac{\partial^2 u_2}{\partial x^2}=-\dfrac{\partial^2\phi_2}{\partial x^2}-\dfrac{q}{\eta}(u_2+\phi_2)\left((u_1+\phi_1)^2+(u_2+\phi_2)^2\right)^{\frac{p}{2}}, \\ u_1(x,0)=u_2(x,0)=0, \\ u_1(a,t)=u_1(b,t)=u_2(a,t)=u_2(b,t)=0. \end{cases} \tag{1}$$

Put

$$A_{11}u_1=\frac{\partial^2 u_1}{\partial x^2}, \qquad A_{12}u_2=-\frac{1}{\eta}\frac{\partial u_2}{\partial t},$$
$$A_{21}u_1=\frac{1}{\eta}\frac{\partial u_1}{\partial t}, \qquad A_{22}u_2=\frac{\partial^2 u_2}{\partial x^2},$$
$$A=\begin{pmatrix} A_{11} & A_{12} \\ A_{21} & A_{22}\end{pmatrix},$$
$$N_1(x,t,u)=-\frac{\partial^2\phi_1}{\partial x^2}-\frac{q}{\eta}(u_1+\phi_1)\left((u_1+\phi_1)^2+(u_2+\phi_2)^2\right)^{\frac{p}{2}},$$
$$N_2(x,t,u)=-\frac{\partial^2\phi_2}{\partial x^2}-\frac{q}{\eta}(u_2+\phi_2)\left((u_1+\phi_1)^2+(u_2+\phi_2)^2\right)^{\frac{p}{2}},$$

then problem (1) can be converted into the following form:

$$\begin{cases} Au=N(x,t,u), \quad (x,t)\in\Omega, \\ u(x,0)=0, \\ u(a,t)=u(b,t)=0, \end{cases} \tag{2}$$

where $u=(u_1,u_2)^T$, $N=(N_1,N_2)^T$, $u\in W(\Omega)\oplus W(\Omega)$, $N\in\widetilde{W}(\Omega)\oplus\widetilde{W}(\Omega)$. The space $W(\Omega)\oplus W(\Omega)$ is defined as

$$W(\Omega)\oplus W(\Omega)=\{u=(u_1,u_2)^T\,|\,\{u_i\}_{i=1}^2\in W(\Omega)\}.$$

The inner product and norm are defined respectively by

$$\langle u,v\rangle=\sum_{i=1}^{2}\langle u_i,v_i\rangle_W, \quad \|u\|=\left(\sum_{i=1}^{2}\|u_i\|^2\right)^{\frac{1}{2}}, \quad \forall u,v\in W(\Omega)\oplus W(\Omega).$$

The space $\widetilde{W}(\Omega)\oplus\widetilde{W}(\Omega)$ can be defined in a similar manner. The reproducing kernel Hilbert spaces $W(\Omega)$ and $\widetilde{W}(\Omega)$ are defined in the following section.

3. Reproducing kernel spaces

Definition 1. Let H be a real Hilbert space of functions $f:\Omega\to\mathbb{R}$. Denote by $\langle\cdot,\cdot\rangle$ the inner product and let $\|\cdot\|=\sqrt{\langle\cdot,\cdot\rangle}$ be the induced norm in H. A complex valued function $K(x,y):\Omega\times\Omega\to\mathbb{R}$ is called a reproducing kernel of H if the following are satisfied:

(i) $K_y(x)=K(x,y)\in H$ for all $y\in\Omega$,
(ii) $f(y)=\langle f(x),K_y(x)\rangle$ for all $f\in H$ and for all $y\in\Omega$.

Definition 2. A Hilbert space H of functions on a set Ω is called a reproducing kernel Hilbert space if there exists a reproducing kernel K of H.

Remark 1. The existence of the reproducing kernel of a Hilbert space H is due to the Riesz Representation Theorem. It is known that the reproducing kernel is unique.

Definition 3. Let $K: \Omega \times \Omega \to C$ be a kernel on Ω. The kernel K is called positive definite, if for any finite set of points $\{y_1, \dots, y_n\}$ and any complex numbers $\varepsilon_1, \dots, \varepsilon_n$ we have

$$\sum_{i,j=1}^{n} \bar{\varepsilon}_i \varepsilon_j K(y_i, y_j) \geq 0.$$

Theorem 1. The reproducing kernel $K_y(x)$ of a reproducing kernel Hilbert space H is positive definite.

It has been proved that for every positive definite kernel K corresponds one and only one class of functions F with a uniquely determined inner product in it, forming a Hilbert space and admitting K as a reproducing kernel. In fact, the kernel K produces the entire space H, i.e.,

$$H = \overline{\text{span}\{K(z,.)|z \in \Omega\}}.$$

We note that it is possible to define several different inner products in the same class of functions H, so that H is complete with respect to each one of the corresponding norms. To each one of the Hilbert spaces $(H, \langle .,. \rangle)$ there corresponds one and only one kernel function K. That is to say K depends not only on the class of functions H, but also on the choice of the inner product that H admits. Now, we define some useful reproducing kernel spaces.

Definition 4. $W_0[a,b] = \{u(x)|u(x), u'(x), u''(x)$ are absolutely continuous in $[a,b], u^{(3)}(x) \in L^2[a,b], u(a) = 0, u(b) = 0\}$. The inner product and the norm in $W_0[a,b]$ are defined respectively by

$$\langle u, v \rangle_{W_0} = u(a)v(a) + u'(a)v'(a) + u(b)v(b) + \int_a^b u^{(3)}(x)v^{(3)}(x)dx, \quad u, v \in W_0[a,b], \tag{3}$$

and

$$\| u \|_{W_0} = \sqrt{\langle u, u \rangle_{W_0}}, \quad u \in W_0[a,b].$$

The space $W_0[a,b]$ is a reproducing kernel space and its reproducing kernel function is $R_y(x)$ given in Appendix.

Definition 5. $W_1[0,T] = \{u(t)|u(t), u'(t)$ are absolutely continuous in $[0,T], u''(t) \in L^2[0,T], u(0) = 0\}$. The inner product and the norm in $W_1[0,T]$ are defined respectively by

$$\langle u, v \rangle_{W_1} = \sum_{i=0}^{1} u^{(i)}(0)v^{(i)}(0) + \int_0^T u''(t)v''(t)dt, \quad u, v \in W_1[0,T],$$

and

$$\| u \|_{W_1} = \sqrt{\langle u, u \rangle_{W_1}}, \quad u \in W_1[0,T].$$

The space $W_1[0,T]$ is a reproducing kernel space and its reproducing kernel function $r_s(t)$ is given by

$$r_s(t) = \begin{cases} st + \frac{s}{2}t^2 - \frac{1}{6}t^3 & t \leq s, \\ st + \frac{s^2}{2}t - \frac{1}{6}s^3 & t > s. \end{cases}$$

Definition 6. $W_2[a,b] = \{u(x)|u(x), u'(x)$ are absolutely continuous in $[a,b], u''(x) \in L^2[a,b]\}$. The inner product and the norm in $W_2[a,b]$ are defined respectively by

$$\langle u, v \rangle_{W_2} = \sum_{i=0}^{1} u^{(i)}(a)v^{(i)}(a) + \int_a^b u''(x)v''(x)dx, \quad u, v \in W_2[a,b],$$

and

$$\| u \|_{W_2} = \sqrt{\langle u, u \rangle_{W_2}}, \quad u \in W_2[a,b].$$

The space $W_2[a,b]$ is a reproducing kernel space and its reproducing kernel function $Q_y(x)$ is given by

$$Q_y(x) = \begin{cases} 1 + yx + \frac{y}{2}x^2 - \frac{1}{6}x^3 & x \leq y, \\ 1 + yx + \frac{y^2}{2}x - \frac{1}{6}y^3 & x > y. \end{cases}$$

Definition 7. $W_3[0,T] = \{u(t)|u(t)$ is absolutely continuous in $[0,T], u'(t) \in L^2[0,T]\}$. The inner product and the norm in $W_3[0,T]$ are defined respectively by

$$\langle u, v \rangle_{W_3} = u(0)v(0) + \int_0^T u'(t)v'(t)dt, \quad u, v \in W_3[0,T],$$

and

$$\| u \|_{W_3} = \sqrt{\langle u, u \rangle_{W_3}}, \quad u \in W_3[0,T].$$

The space $W_3[0,T]$ is a reproducing kernel space and its reproducing kernel function $q_s(t)$ is given by

$$q_s(t) = \begin{cases} 1+t & t \le s, \\ 1+s & t > s. \end{cases}$$

Definition 8. $W(\Omega) = \{u(x,t) | \frac{\partial^3 u}{\partial x^2\, \partial t}$ is completely continuous in Ω, $\frac{\partial^5 u}{\partial x^3\, \partial t^2} \in L^2(\Omega), u(x,0) = 0, u(a,t) = 0, u(b,t) = 0\}$. The inner product and the norm in $W(\Omega)$ are defined respectively by

$$\begin{aligned} \langle u, v\rangle_W &= \sum_{i=0}^{1} \int_0^T \left[\frac{\partial^2}{\partial t^2}\frac{\partial^i}{\partial x^i}u(a,t)\frac{\partial^2}{\partial t^2}\frac{\partial^i}{\partial x^i}v(a,t)\right]dt \\ &+ \sum_{j=0}^{1} \langle \frac{\partial^j}{\partial t^j}u(x,0), \frac{\partial^j}{\partial t^j}v(x,0)\rangle_{W_0} \\ &+ \int_0^T \int_a^b \left[\frac{\partial^3}{\partial x^3}\frac{\partial^2}{\partial t^2}u(x,t)\frac{\partial^3}{\partial x^3}\frac{\partial^2}{\partial t^2}v(x,t)\right]dxdt, \\ & u, v \in W(\Omega), \end{aligned}$$

and

$$\| u \|_W = \sqrt{\langle u, u\rangle_W}, \quad u \in W(\Omega).$$

Theorem 2. $W(\Omega)$ is a reproducing kernel space and its reproducing kernel function is

$$K_{(y,s)}(x,t) = R_y(x) r_s(t),$$

such that for any $u(x,t) \in W(\Omega)$,

$$u(y,s) = \langle u(x,t), K_{(y,s)}(x,t)\rangle_W,$$

and

$$K_{(y,s)}(x,t) = K_{(x,t)}(y,s),$$

where $R_y(x)$, $r_s(t)$ are the reproducing kernel functions of $W_0[a,b]$ and $W_1[0,T]$, respectively.

Proof: See [43].

Definition 9. $\widetilde{W}(\Omega) = \{u(x,t) | \frac{\partial u}{\partial x}$ is completely continuous in Ω, $\frac{\partial^3 u}{\partial x^2\, \partial t} \in L^2(\Omega)\}$. The inner product and the norm in $\widetilde{W}(\Omega)$ are defined respectively by

$$\begin{aligned} &\langle u(x,t), v(x,t)\rangle_{\widetilde{W}} \\ &= \sum_{i=0}^{1} \int_0^T \left[\frac{\partial}{\partial t}\frac{\partial^i}{\partial x^i}u(0,t)\frac{\partial}{\partial t}\frac{\partial^i}{\partial x^i}v(0,t)\right]dt \\ &+ \langle u(x,0), v(x,0)\rangle_{W_2} \\ &+ \int_0^T \int_a^b \left[\frac{\partial^2}{\partial x^2}\frac{\partial}{\partial t}u(x,t)\frac{\partial^2}{\partial x^2}\frac{\partial}{\partial t}v(x,t)\right]dxdt, \\ & u, v \in \widetilde{W}(\Omega), \end{aligned}$$

and

$$\| u \|_{\widetilde{W}} = \sqrt{\langle u, u\rangle_{\widetilde{W}(\Omega)}}, \quad u \in \widetilde{W}(\Omega).$$

$\widetilde{W}(\Omega)$ is a reproducing kernel space and its reproducing kernel function is

$$G_{(y,s)}(x,t) = Q_y(x) q_s(t).$$

4. The method implementation

In this section, we will give the representation of analytical and approximate solution of (2) in the reproducing kernel space $W(\Omega) \oplus W(\Omega)$. At first the following lemma is given.

Lemma 1. If $A_{ij}: W(\Omega) \to W(\Omega)$, $i, j = 1,2$, are bounded linear operators, then $A: W(\Omega) \oplus W(\Omega) \to W(\Omega) \oplus W(\Omega)$ is a bounded linear operator.

Proof: See [42].
It is easy to show that the adjoint operator of A is

$$A^* = \begin{pmatrix} A_{11}^* & A_{21}^* \\ A_{12}^* & A_{22}^* \end{pmatrix},$$

where A_{ij}^* is the adjoint operator of A_{ij}. Now let $\{(x_i, t_i)\}_{i=1}^{\infty}$ be a countable dense subset in Ω, and define

$$\phi_{ij}(x,t) = G_{(x_i,t_i)}(x,t)\vec{e_j} = \begin{cases} \left(G_{(x_i,t_i)}(x,t), 0\right)^T & j = 1, \\ \left(0, G_{(x_i,t_i)}(x,t)\right)^T & j = 2, \end{cases}$$

$$\psi_{ij}(x,t) = A^* \phi_{ij}(x,t), i = 1,2,\dots,\infty, j = 1,2$$

where A^* is the adjoint operator of A.

Theorem 3. Suppose that $\{(x_i, t_i)\}_{i=1}^{\infty}$ is dense in Ω. Then $\{\psi_{ij}(x,t)\}_{(1,1)}^{(\infty,2)}$ is a complete system in $W(\Omega) \oplus W(\Omega)$ and $\psi_{ij}(x,t) = A_{(y,s)}(K_{(y,s)}(x,t)\vec{e_j})|_{(y,s)=(x_i,t_i)}$.

Proof: We have

$$\begin{aligned} &\psi_{ij}(x,t) = A^* \phi_{ij}(x,t) \\ &= \sum_{j=1}^{2} \langle A^* \phi_{ij}(y,s), K_{(x,t)}(y,s)\vec{e_j}\rangle \vec{e_j} \\ &= \sum_{j=1}^{2} \langle \phi_{ij}(y,s), A_{(y,s)} K_{(x,t)}(y,s)\vec{e_j}\rangle \vec{e_j} \\ &= A_{(y,s)}(K_{(x,t)}(y,s)\vec{e_j})|_{(y,s)=(x_i,t_i)} \\ &= A_{(y,s)}(K_{(y,s)}(x,t)\vec{e_j})|_{(y,s)=(x_i,t_i)}. \end{aligned}$$

If

$$\langle u(x,t), \psi_{ij}(x,t)\rangle = 0, \quad i = 1,2\dots,\infty, \quad j = 1,2$$

then

$$\langle u(x,t), A^*\phi_{ij}(x,t)\rangle = \langle Au(x,t), \phi_{ij}(x,t)\rangle = 0.$$

Thus

$$Au(x_i,t_i) = \sum_{j=1}^{2} \langle Au(y,s), \phi_{ij}(y,s)\rangle \vec{e_j} = 0.$$

Note that $\{(x_i,t_i)\}_{i=1}^{\infty}$ is dense in Ω, hence, $(Au)(x,t) = 0$. It follows that $u \equiv 0$ from the existence of A^{-1}. So the proof is complete.
In the sequel, we give the analytical and approximate solutions of the operator equation (2) in the reproducing kernel space.

Theorem 4. Suppose that $\{(x_i,t_i)\}_{i=1}^{\infty}$ is dense in Ω, then the analytical solution of (2) can be represented as

$$u(x,t) = \sum_{l=1}^{\infty} \sum_{k=1}^{2} N_k(x_l,t_l,u(x_l,t_l))\xi_{lk}(x,t) \quad (4)$$

where the vectors $\xi_1 = [\xi_{11}(x,t), \xi_{21}(x,t), \dots]^T$ and $\xi_2 = [\xi_{12}(x,t), \xi_{22}(x,t), \dots]^T$ can be obtained by

$$B_1\xi_1 = \psi_1, \quad (5)$$

$$B_2\xi_2 = \psi_2, \quad (6)$$

where

$$B_k = \left[A\psi_{jk}(x,t)|_{(x,t)=(x_i,t_i)}\right]_{i,j=1,2,\dots}$$
$$\psi_1 = [\psi_{11}(x,t), \psi_{21}(x,t), \dots]^T, \quad \psi_2 = [\psi_{12}(x,t), \psi_{22}(x,t), \dots]^T.$$

Proof: Since $\{(x_i,t_i)\}_{i=1}^{\infty}$ is dense in Ω, it is enough to show that

$$Au(x_i,t_i) = N(x_i,t_i,u(x_i,t_i)), \qquad i = 1, \dots, \infty.$$

So

$$Au(x_i,t_i) = \sum_{j=1}^{2} \langle Au(x,t), \phi_{ij}(x,t)\rangle \vec{e_j} = \sum_{j=1}^{2} \langle u(x,t), A^*\phi_{ij}(x,t)\rangle \vec{e_j}$$
$$= \sum_{j=1}^{2} \langle \sum_{l=1}^{\infty} \sum_{k=1}^{2} N_k(x_l,t_l,u(x_l,t_l))\xi_{lk}(x,t), A^*\phi_{ij}(x,t)\rangle \vec{e_j}$$
$$= \sum_{j=1}^{2} \langle \sum_{l=1}^{\infty} \sum_{k=1}^{2} N_k(x_l,t_l,u(x_l,t_l))A\xi_{lk}(x,t), \phi_{ij}(x,t)\rangle \vec{e_j}$$
$$= \sum_{l=1}^{\infty} \sum_{k=1}^{2} N_k(x_l,t_l,u(x_l,t_l))A\xi_{lk}(x,t)|_{(x,t)=(x_i,t_i)}$$

Now, since the matrix $\left[A\xi_{lk}(x,t)|_{(x,t)=(x_i,t_i)}\right]_{\substack{i,l=1,2,\dots \\ k=1,2}}$ is an identity matrix, we have

$$A\xi_{lk}(x,t)|_{(x,t)=(x_i,t_i)} = \begin{cases} (1,0)^T & k=1, i=l, \\ (0,1)^T & k=2, i=l, \\ (0,0)^T & i \neq l. \end{cases}$$

So

$$Au(x_i,t_i) = N_1(x_i,t_i,u(x_i,t_i))(1,0)^T + N_2(x_i,t_i,u(x_i,t_i))(0,1)^T = N(x_i,t_i,u(x_i,t_i)).$$

Using the initial function $u_0(x,t) = (u_{1,0}(x,t), u_{2,0}(x,t))^T$, the following approximate solution is constructed

$$u_n(x,t) = \sum_{l=1}^{\infty} \sum_{k=1}^{2} N_k(x_l,t_l,u_{n-1}(x_l,t_l))\xi_{lk}(x,t), \quad n = 1,2,\dots. \quad (7)$$

Now, we will prove the convergence of $u_n(x,t)$ to the analytical solution $u(x,t)$ given by (4).

Theorem 5. Suppose that for each $v = (v_1,v_2), \tilde{v} = (\tilde{v}_1,\tilde{v}_2)$ in $W(\Omega) \oplus W(\Omega)$,

$$\| N(x,t,v) - N(x,t,\tilde{v}) \|_{\widetilde{W}(\Omega)\oplus\widetilde{W}(\Omega)} \leq C \| v - \tilde{v} \|_{W(\Omega)\oplus W(\Omega)},$$

and $C \| A^{-1} \| < 1$, then $u_n \overset{\|.\|}{\to} u$, as $n \to \infty$.

Proof: From Theorem 4,

$$Au(x,t) = N(x,t,u(x,t)), \quad Au_n(x,t) = N(x,t,u_{n-1}(x,t)).$$

So

$$\| u_n(x,t) - u(x,t) \| = \| A^{-1}(N(x,t,u_{n-1}(x,t)) - N(x,t,u(x,t)) \| \leq \| A^{-1} \| . \| N(x,t,u_{n-1}(x,t)) - N(x,t,u(x,t)) \| \leq C \| A^{-1} \| . \| u_{n-1}(x,t) - u(x,t) \|.$$

Therefore $u_n \overset{\|.\|}{\to} u$, as $n \to \infty$.

Theorem 6. If $u_n(x,t) \overset{\|.\|}{\to} u(x,t)$, then $u_n(x,t) \to u(x,t)$, as $n \to \infty$.

Proof: Since

$$|u_n(x,t) - u(x,t)| = |\langle u_n(\zeta,\eta) - u(\zeta,\eta), K_{(x,t)}(\zeta,\eta)\rangle| \leq \| u_n(\zeta,\eta) - u(\zeta,\eta) \| \| K_{(x,t)}(\zeta,\eta) \| \leq C_1 \| u_n(\zeta,\eta) - u(\zeta,\eta) \|.$$

Hence $u_n(x,t) \to u(x,t)$, as $n \to \infty$.

Now, by choosing two nonnegative integers n and m, the following computable approximate solution can be obtained by taking finite terms in (7),

$$u_{n,m}(x,t) = \sum_{l=1}^{m} \sum_{k=1}^{2} N_k\big(x_l, t_l, u_{n-1,m}(x_l,t_l)\big)\xi_{lk}(x,t).$$

In this case B_1 and B_2 are a $2m * 2m$ matrix and ψ_1, ψ_2, ξ_1 and ξ_2 are $2m * 1$ vectors.

Remark 2. There exists a unique solution for equations (5) and (6) due to the strictly positive definiteness property of the reproducing kernel.

5. Numerical results

In this section, we present some numerical examples to test the accuracy of our scheme. The set of points in the region $\overline{\Omega}$, are defined by

$$x_i = a + \frac{b-a}{N_1} i, \qquad i = 0, \dots, N_1$$
$$t_i = \frac{T}{N_2} i, \qquad i = 0, \dots, N_2$$

where N_1 and N_2 are the number of interior points in the spatial and time domains, respectively, and $m = (N_1 + 1) \times (N_2 + 1)$. The accuracy of the method is measured by using the maximum error norm

$$L_\infty = \| u - \tilde{u} \| = \max_j |u_j - \tilde{u}_j|,$$

where u and $\tilde{u}$ are the exact and approximate solutions, respectively. The pointwise rate of convergence in space and time are calculated by using the following formulae:

$$\frac{\ln\left(\frac{E(N_{1,i+1})}{E(N_{1,i})}\right)}{\ln\left(\frac{N_{1,i}}{N_{1,i+1}}\right)}, \quad and \quad \frac{\ln\left(\frac{E(N_{2,i+1})}{E(N_{2,i})}\right)}{\ln\left(\frac{N_{2,i}}{N_{2,i+1}}\right)},$$

where $E(N_{1,i})$ and $E(N_{2,i})$ are the norm of the relative errors of the solution with number of spatial points $N_{1,i}$ and number of time points $N_{2,i}$, respectively, where the norm of the relative errors of the solution is defined by

$$L_r = \left(\frac{\sum_{i=1}^{N_1} (u_i - \tilde{u}_i)^2}{\sum_{i=1}^{N_1} {u_i}^2}\right)^{1/2},$$

where u and $\tilde{u}$ are the exact and approximate solutions, respectively. The NLSE has an infinite number of conservation laws including

$$Q = \int_{-\infty}^{\infty} |u|^2 dx \simeq \int_a^b |\tilde{u}|^2 dx,$$
$$E = \int_{-\infty}^{\infty} \left(\eta \left|\frac{\partial u}{\partial x}\right|^2 - \frac{2q}{p+2}|u|^{p+2}\right) dx \simeq \int_a^b \left(\eta \left|\frac{\partial \tilde{u}}{\partial x}\right|^2 - \frac{2q}{p+2}|\tilde{u}|^{p+2}\right) dx,$$

corresponding to the conservation laws of charge and energy, respectively. Relative errors of invariants are defined by

$$\overline{Q} = \frac{Q - Q_0}{Q_0},$$
$$\overline{E} = \frac{E - E_0}{E_0},$$

where E_0 and Q_0 are the values of Q and E at the time $T = 0$, respectively. To test the accuracy of the proposed method, two examples are treated in this section.

Example 1. (**The linear Schrödinger equation**) Consider the linear Schrödinger equation

$$i\,\frac{\partial u}{\partial t} + \eta \frac{\partial^2 u}{\partial x^2} + qu = 0.$$

The exact solution is given by

$$u(x,t) = \alpha \exp(\, i\,(q - 4\eta k^2 \pi^2)t) \sin(2k\pi x).$$

We work with the parameters $a = 0$, $b = 1$, $n = 5$, $q = \frac{1}{2}$, and $\alpha = \eta = k = 1$. The absolute errors of $|u(x,\mathrm{t})|$ for $t = \frac{1}{2}$ are shown in Fig. 1, with different values of the parameter m. The numerical invariant values are plotted in Fig. 2, with $m = 100$, which shows that our method preserves the two conservation laws. The curves of real and imaginary parts of the numerical and exact solutions at different times are shown in Fig. 3, with $m = 100$, which indicate that they are in good agreement. In order to examine the pointwise rate of convergence in space and time, computations are carried out with the different number of spatial and time points. In Table 1, the number of time points is kept fixed at $N_2 = 20$ and the number of spatial points $N_1 = 2,4,8,16,32$ is varied to calculate the spatial rate of convergence. It can be noted from Table 1, that the rate of convergence increases with the larger number of spatial points. In Table 2, the number of spatial points is kept fixed at $N_1 = 20$ and the number of time points $N_2 = 2,4,8,16,32$ is varied to compute the time rate of convergence. It can be noted from Table 2, that the rate of

convergence increases with the larger number of time points.

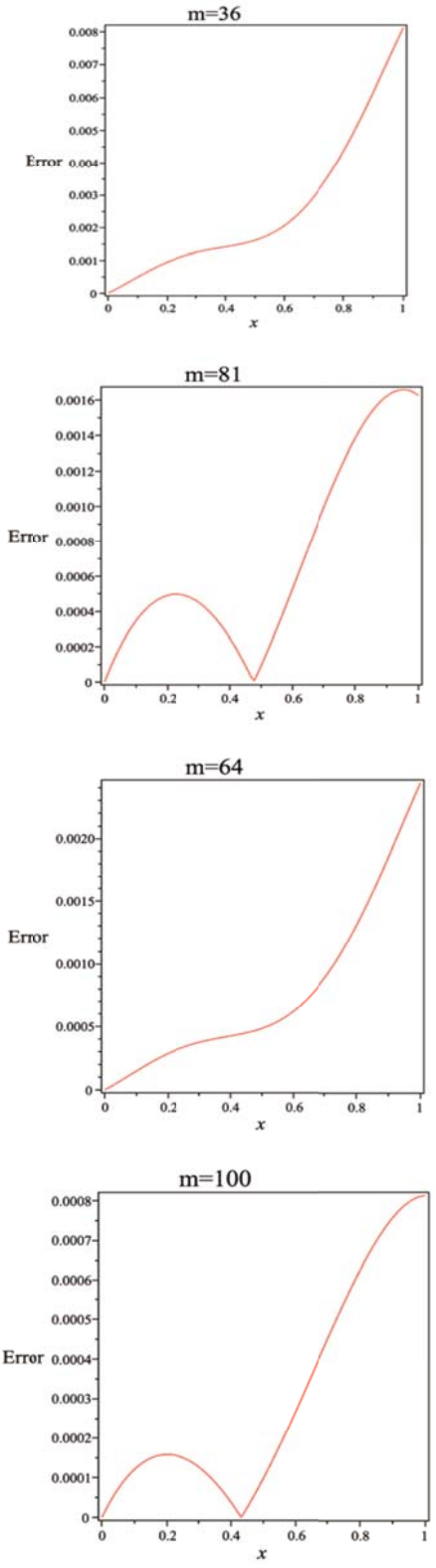

Fig. 1. Absolute errors of $|\boldsymbol{u}(\boldsymbol{x},\frac{\mathbf{1}}{\mathbf{2}}) - \boldsymbol{u}_{\mathbf{5},\boldsymbol{m}}(\boldsymbol{x},\frac{\mathbf{1}}{\mathbf{2}})|$, for the linear Schrödinger equation

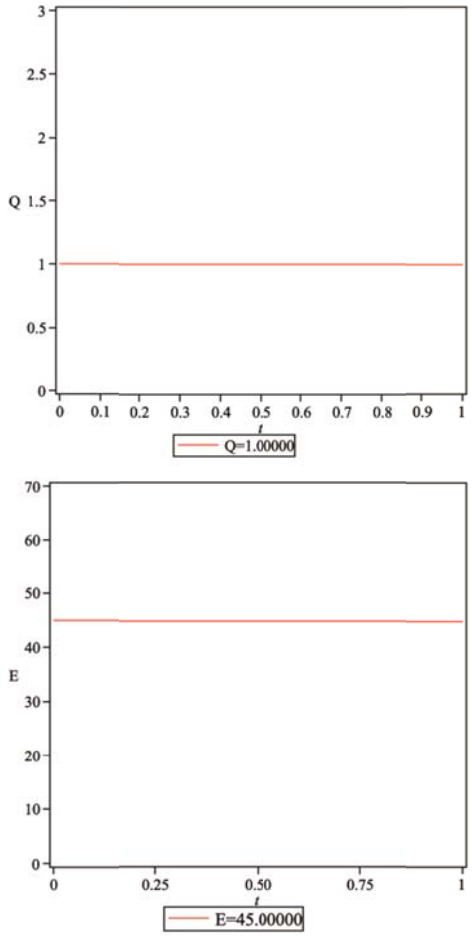

Fig. 2. The numerical charge ($\boldsymbol{Q}$) and energy ($\boldsymbol{E}$) for the linear Schrödinger equation from $\boldsymbol{t = 0}$ to $\mathbf{1}$ with $\boldsymbol{m = 100}$

Table 1. Spatial rate of convergence for the linear Schrödinger equation at $\mathbf{T} = \frac{\mathbf{1}}{\mathbf{2}}$, $\mathbf{N_2 = 20}$

N_1	L_r	Order
2	2.110038E-02	-
4	8.522371E-03	1.307942
8	2.913090E-03	1.548705
16	8.233013E-04	1.823058
32	2.121349E-04	1.956438

Table 2. Time rate of convergence for the for the linear Schrödinger equation at $\mathbf{T} = \frac{\mathbf{1}}{\mathbf{2}}$, $\mathbf{N_1 = 20}$

N_2	L_r	Order
2	1.330025E-02	-
4	7.392653E-03	0.847289
8	3.514223E-03	1.072886
16	1.211148E-03	1.536831
32	3.699890E-04	1.710817

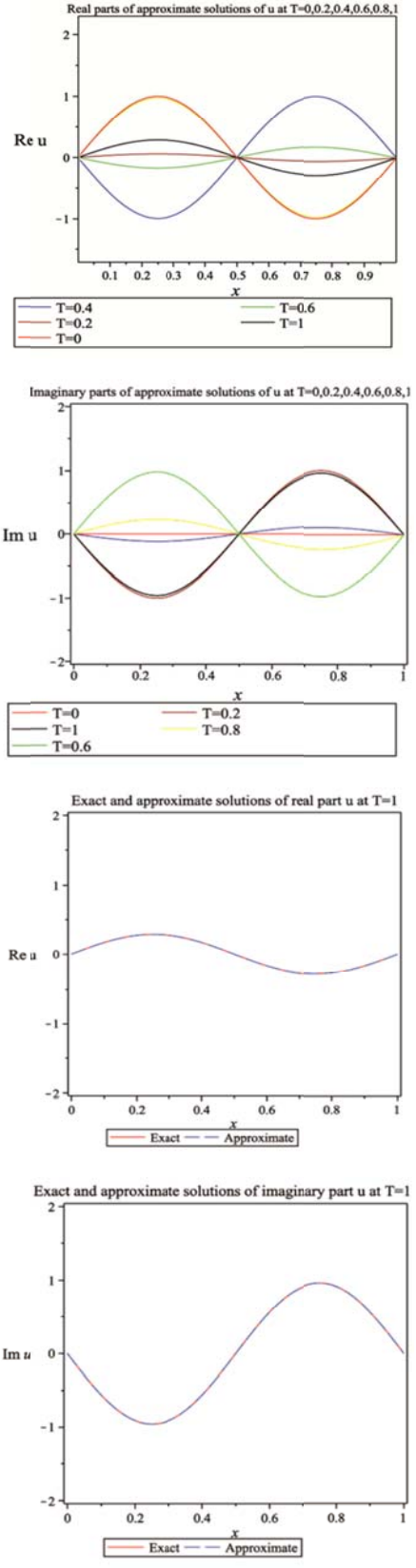

Fig. 3. The real and imaginary parts of the numerical and exact solutions of the linear Schrödinger equation from $t = 0$ to $t = 1$

Example 2. (The cubic nonlinear Schrödinger equation)

I) One-soliton solution

Consider the cubic nonlinear Schrödinger equation

$$i\frac{\partial u}{\partial t} + \eta\frac{\partial^2 u}{\partial x^2} + q|u|^2 u = 0.$$

It has the following single soliton solution

$$u(x,t) = \alpha\left(\frac{2}{q}\right)^{\frac{1}{2}} \exp i\left(\frac{1}{2}sx - \frac{1}{4}(s^2 - \alpha^2)t\right) sech\,(\alpha(x - st)),$$

where s represents the speed of the soliton and its magnitude depends on α. We work with the parameters $a = -20$, $b = 20$, $\eta = \alpha = 1$, $s = 4$, $q = 2$ in order to make comparison with analytical solutions and earlier studies [28, 31, 32, 33, 37]. The absolute errors of $|u(x,t)|$ for $t = 1$ are shown in Fig. 4, with $n = 5$ and different values of the parameter m. The numerical invariant values are also plotted in Fig. 5, with $m = 100$, which shows that the numerical invariant values are almost constant during the simulation. The modulus of the exact and numerical solutions with $m = 100$ at different times is shown in Fig. 6 and the curves of real and imaginary parts of those solutions are drawn in Fig. 7, which indicate that they are in good agreement. The calculated L_∞ error norms and the conserved quantities Q and E in addition to their relative errors at time $T = 1$ are tabulated in Table 3. The analytical values of the invariants are $Q = 2$ and $E = 7.333333$. It can be seen from Table 3 that the numerical invariants are completely equal to the analytical ones, in our method. The L_∞ error norms corresponding to our method are in agreement with the reported ones in [31, 37], but better than the results of [28, 32].

II) Interaction of two solitary waves

We consider the interaction of two solitary waves. The initial and boundary conditions are given by

$$u(x,0) = sech\,(x)\exp(2\,i\,x) + sech\,(x - 10)\exp(0.01\,i\,(x - 10)),$$

and

$$u(-10,t) = u(30,t) = 0.$$

This initial condition yields a two-soliton solution, where the solitons are separated by a distance of 10 units at $t = 0$. As time progresses, the faster soliton eventually catches up with the slower one and, according to the soliton theory, passes through it with only a phase shift resulting from the collision. Our numerical experiment is conducted from time $t = 0$ to 5 with $m = 100$ and $n = 5$. The evolution of the two invariants is given in Fig. 8, which shows that our method preserves the conservation laws for charge and energy.

During our simulations, the charge $\boldsymbol{Q}$ seems to remain constant value $\boldsymbol{Q = 4}$ all the time, whereas the energy $\boldsymbol{E}$ changes slightly when the solitons interact and then $\boldsymbol{E}$ becomes constant value $\boldsymbol{E = 6.51000}$ again after the interaction. The modulus and the real and imaginary parts of the numerical solution are drawn in Figs. 9 and 10, respectively. In our numerical experiment the two solitons collide but recover their shapes afterwards despite a strongly nonlinear interaction. These results are in qualitative agreement with the behavior predicted by the soliton theory [44, 45, 46]. In the second experiment, collision of two solitons is studied with the initial condition

$$\boldsymbol{u(x,0) = u_1(x,0) + u_2(x,0),}$$

where

$$\boldsymbol{u_j(x,0) = \alpha_j \left(\frac{2}{q}\right)^{\frac{1}{2}} \exp i \left(\frac{1}{2} s(x - x_j)\right) sech\left(\alpha_j (x - x_j)\right), j = 1, 2.}$$

By taking $\boldsymbol{q = 2}$, $\boldsymbol{\alpha_1 = 1}$, $\boldsymbol{s_1 = 4}$, $\boldsymbol{x_1 = -10}$, $\boldsymbol{\alpha_2 = 1}$, $\boldsymbol{s_2 = -4}$, $\boldsymbol{x_2 = 10}$, $\boldsymbol{m = 100}$, and $\boldsymbol{n = 5}$ over the region $\boldsymbol{-20 < x < 20}$, numerical values of invariants in addition to their relative errors at time $\boldsymbol{T = 5}$ are given in Table 4. The analytical values of invariants are $\boldsymbol{Q = 4}$ and $\boldsymbol{E = 14.6666666667}$. It is clear that the invariants are conserved as time increases. The relative errors of invariants in our method are slightly smaller than the reported ones in [28, 31, 32, 37].

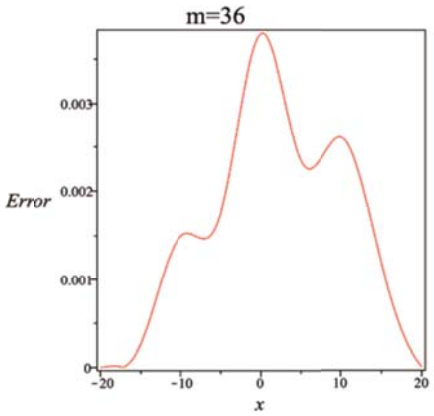

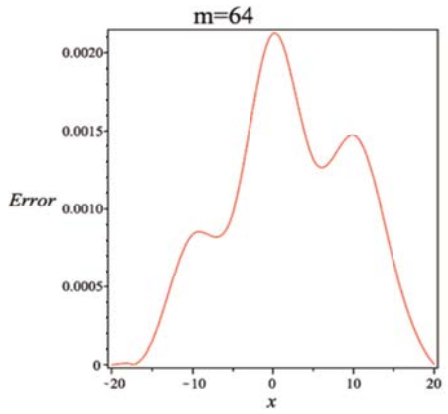

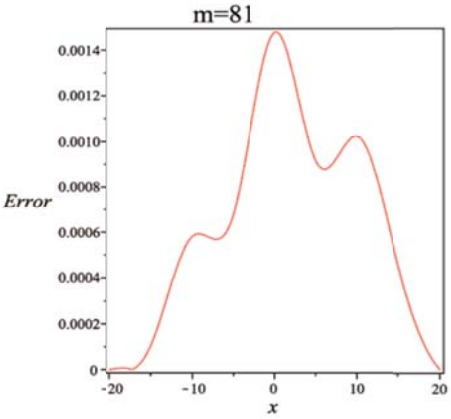

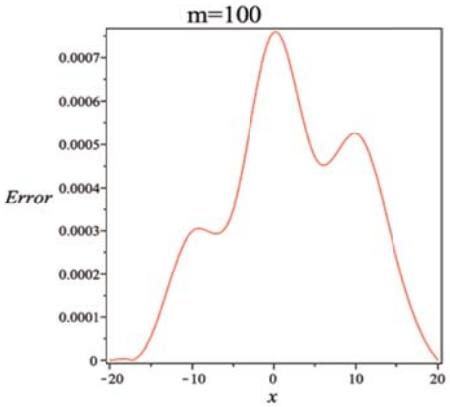

Fig. 4. Absolute errors of $|\boldsymbol{u(x,1) - u_{5,m}(x,1)}|$, for the one-soliton solution of the cubic NLSE

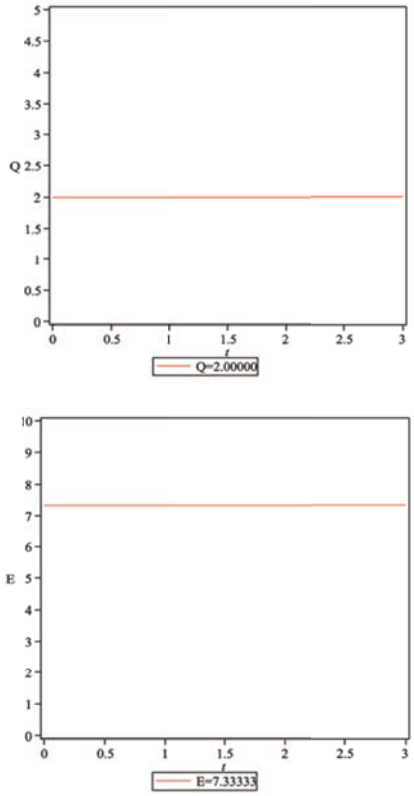

Fig. 5. The numerical charge ($\boldsymbol{Q}$) and energy ($\boldsymbol{E}$) for the one-soliton solution of the cubic NLSE from $\boldsymbol{t = 0}$ to $\boldsymbol{3}$ with $\boldsymbol{m = 100}$

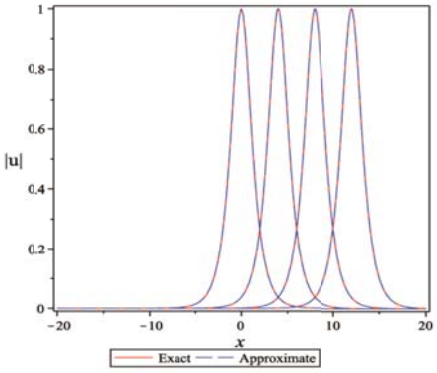

Fig. 6. The modulus of numerical and exact solutions of the one-soliton solution of the cubic NLSE from $\boldsymbol{t = 0}$ to $\boldsymbol{t = 3}$

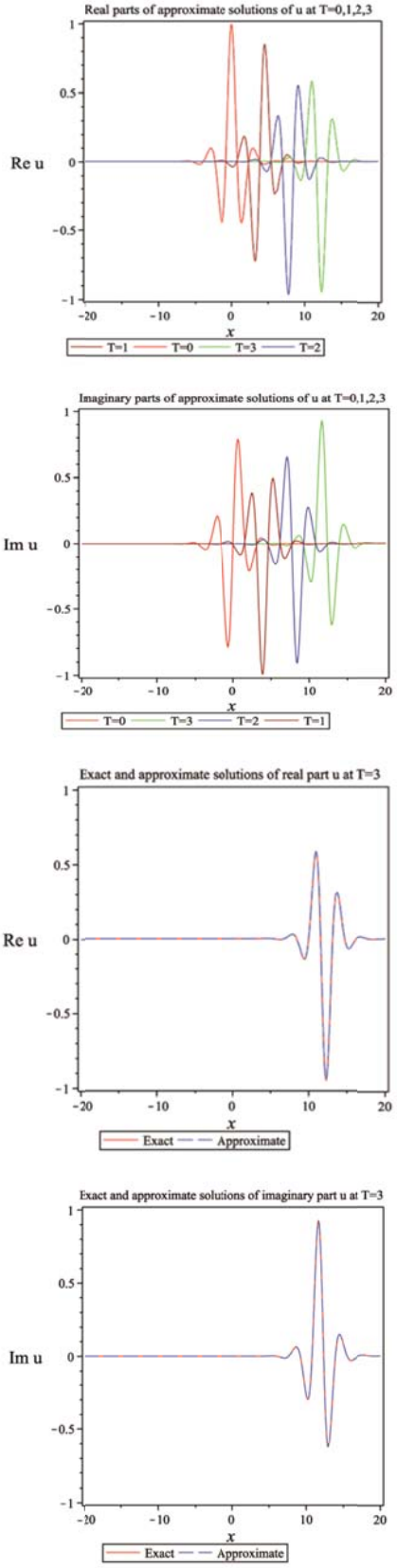

Fig. 7. The real and imaginary parts of the numerical and exact solutions of the one-soliton solution of the cubic NLSE from $\boldsymbol{t = 0}$ to $\boldsymbol{t = 3}$

Table 3. Comparison of error norms and relative error of invariants at time $\mathbf{T} = \mathbf{1}$

Method	Parameters	L_∞	Q	E	$\overline{Q}$	$\overline{E}$
RKS (present)	$n = 5$ $m = 400$	1.021000E-06	2.00000000	7.33333333	0.000000	0.000000
[37]G	$h = 0.3125$ $\Delta t = 0.02$	1.668400E-06	2.00000000	7.33333332	2.559900E-12	-1.650000E-09
[37]MQ	$h = 0.3125$ $\Delta t = 0.02$	1.874100E-06	1.99999999	7.33333319	4.078000E-09	-1.855700E-08
[37]W(7,5)	$h = 0.3125$ $\Delta t = 0.02$	7.228600E-06	1.99999999	7.33333222	-2.555000E-11	-1.509400E-07
[28]	$h = 0.3125$ $\Delta t = 0.02$	2.000000E-03	-	-	6.600000E-06	-3.417000E-04
[32]	$h = 0.3125$ $\Delta t = 0.02$	2.531700E-05	-	-	-1.440300E-06	-3.941900E-06
[31]	$h = 0.3125$ $\Delta t = 0.01$	2.089000E-06	1.99900000	7.33300000	-4.512000E-08	-1.253000E-07
RKS (present)	$n = 6$ $m = 441$	3.041011E-07	2.00000000	7.33333333	0.000000	0.000000
[37]G	$h = 0.1$ $\Delta t = 0.0025$	8.114500E-08	1.99999999	7.33333333	-9.050500E-13	-6.914400E-13
[37]MQ	$h = 0.1$ $\Delta t = 0.0025$	2.898400E-07	2.00000000	7.33333329	8.574000E-11	-5.692900E-09
[37]W(7,5)	$h = 0.1$ $\Delta t = 0.0025$	5.189700E-08	1.99999999	7.33333331	-2.165100E-09	-2.467700E-09
[32]	$h = 0.1$ $\Delta t = 0.0025$	1.932000E-07	1.99999999	7.33333335	-5.222200E-11	2.930600E-09

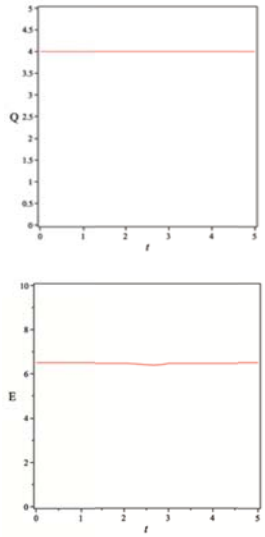

Fig. 8. The numerical charge ($\boldsymbol{Q}$) and energy ($\boldsymbol{E}$) for the interaction of two solitary waves of the cubic NLSE from $\boldsymbol{t = 0}$ to $\mathbf{5}$ with $\boldsymbol{m = 100}$

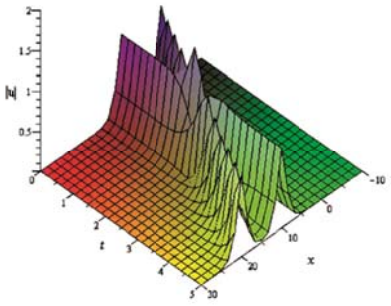

Fig. 9. The modulus of numerical solutions of the interaction of two solitary waves of the cubic NLSE from $\boldsymbol{t = 0}$ to $\boldsymbol{t = 5}$

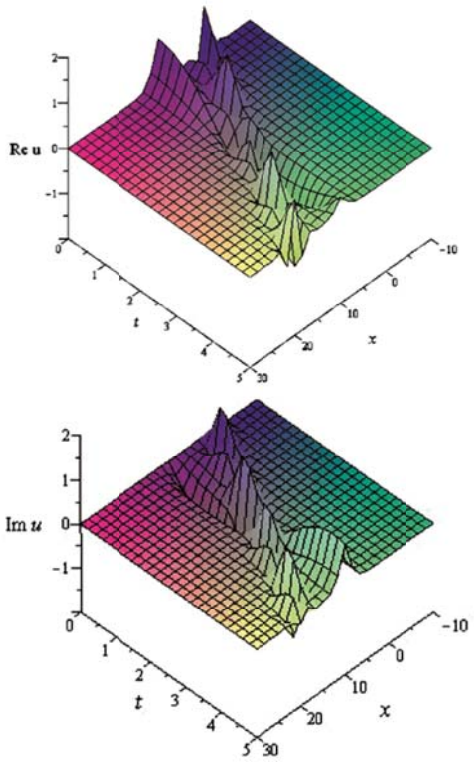

Fig. 10. The real and imaginary parts of numerical solutions of the interaction of two solitary waves of the cubic NLSE from $\boldsymbol{t = 0}$ to $\boldsymbol{t = 5}$

Table 4. Comparison of invariants and relative error of invariants at time $\mathbf{T = 5}$

Method	Parameters	Q	E	$\overline{Q}$	$\overline{E}$
RKS (present)	$n = 5$ $m = 400$	4.0000000121	14.6666659644	3.0250000000E-09	-4.7884000000E-08
[37]G	$h = 0.25$ $\Delta t = 0.01$	4.0000003174	14.6666657344	7.9349999904E-08	-6.3563863627E-08
[37]MQ	$h = 0.25$ $\Delta t = 0.01$	4.0000003175	14.6666620288	7.9374999906E-08	-3.1621840915E-07
[37]W(7,5)	$h = 0.25$ $\Delta t = 0.01$	4.0000003174	14.6666664743	7.9349999904E-08	-1.3116136419E-08
[31]	$h = 0.25$ $\Delta t = 0.01$	3.9999991015	14.6666577117	-	-
[32]	$h = 0.25$ $\Delta t = 0.01$	3.9999991036	14.6666616240	-2.215067637E-07	-4.3588854792E-07
[28]	$h = 0.1$ $\Delta t = 0.01$	3.9999900000	14.8315300000	-	-

6. Conclusion

A new method on the basis of reproducing kernel Hilbert spaces with reasonable accuracy is presented for the 1-D Shrödinger equations. Numerical experiments presented for the linear Shrödinger and the cubic nonlinear Shrödinger equations show that our method is of satisfactory accuracy, preserves the conservation laws of charge and energy, and successfully simulates the physical behaviors of the motion of a single soliton and a two-soliton solution. The advantages of the approach lie in the following facts. The method is mesh free, easily implemented and capable of treating various boundary conditions. The method needs no time discretization against [33] and any ODE integrator against [31, 32, 33]. Also, we can evaluate the approximate solution $\boldsymbol{u_{n,m}(x,t)}$ for fixed $\boldsymbol{n}$ and $\boldsymbol{m}$ once, and use it over and over. The approximate solution also converges uniformly to the analytical solution. The main disadvantage of the method is that it can not handle the high dimensional PDEs with irregular regions because it needs to work with the tensor product of the reproducing kernel spaces corresponding to each dimension. However, the methods [33, 37] use radial basis functions as kernel functions and hence they do not have this disadvantage.

References

[1] Mokhtari, R. & Mohammadi, M. (2009). New exact solutions to a class of coupled nonlinear PDEs. *Int. J. Nonlinear Sci. Numer. Simul*., *10*, 779-796.

[2] Kazemi, M. & Erjaee, G. H. (2011). Analytical and numerical solutions of different parabolic heat equations presented in the form of multi-term fractional differential equations. *IJST-Trans. A, A3*, 185-192.

[3] Mokhtari, R. & Mohammadi, M. (2010). Numerical solution of GRLW equation using Sinc-collocation method. *Comput. Phys. Comm*., *181*, 1266-1274.

[4] Dág, I., Irk, D. & Sahin, A. (2005). B-spline Collocation Method for Numerical Solutions of the Burgers' Equation. *Math. Probl. Eng*., *5*, 521-538.

[5] Dág, I. & Sahin, A. (2007). Solution of the Burgers' Equation Over Geometrically Graded Mesh. *Kybernetes*., *36*, 721-735.

[6] Dág, I., Sahin, A. & Korkmaz, A. (2010). Numerical investigation of the solution of Fisher's equation via the B-spline Galerkin method. Numer. *Methods Partial Differential Equations*., *26*, 1483-1503.

[7] Korkmaz, A. & Dág, I. (2011). Shock wave simulations using Sinc Differential Quadrature *Method. Eng. Computation*., *28*, 564-674.

[8] Korkmaz, A. (2010). Numerical Algorithms for solutions of Korteweg-de Vries Equation. *Numer. Meth. Part, D. E*., *26*, 1504-1521.

[9] Korkmaz A. & Dág, I. (2009). Crank-Nicolson-Differential Quadrature Algoritms for the Kawahara equation. *Chaos Soliton Fract*., *42*, 65-73.

[10] Korkmaz A. & Dág, I. (2009). Solitary Wave Simulations of Complex Modified Korteweg-de Vries Equation using Differential Quadrature Method. Comput. *Phys. Comm*., *180*, 1516-1523.

[11] Davydov, A. S. (1985). *Solitons in Molecular System*. Reidel, Dordrecht.

[12] Dodd, R. K., Eilbeck, J. C., Gibbon, J. D. & Morris, H. C. (1982). *Solitons and Nonlinear Wave Equations*. New York, Academic Press.

[13] Hasegawa, A. (1989). Optical Solitons in Fibers. Berlin, Springer-Verlag.

[14] Sulem, C. & Sulem, P. L. (1999). The Nonlinear Schrödinger Equation Self-focusing and Wave Collapse. New York, Springer.

[15] Ablowitz, M. J. & Segur, H. (1981). *Solitons and the Inverse Scattering Transform*. SIAM, Philadelphia, PA.

[16] Taha, T. R. (1991). A numerical scheme for the nonlinear Schrödinger equation. Comput. *Math. Appl*., *22*, 77-84.

[17] Taha, T. R. (1996). Inverse scattering transform numerical schemes for nonlinear evolution equations and the method of lines. *Appl. Numer. Math*., *20*, 181-187.

[18] Chang, Q., Jia, E. & Sun, W. (1999). Difference schemes for solving the generalized nonlinear Schrödinger equation. *J. Comput. Phys. 148*, 397-415.

[19] Delfour, M., Fortin, M. & Payre, G. (1981). Finite difference solution of a nonlinear Schrödinger equation. *J. Comput. Phys*., *44*, 277-288.

[20] Sanz-Serna, J. M. (1984). Methods for the numerical solution of the nonlinear Schrödinger equation. *Math. Comput*., *43*, 21-27.

[21] Taha, T. R. & Ablowitz, M. J. (1984). Analytical and numerical aspects of certain nonlinear evolution equations: II. Numerical nonlinear Schrödinger equation. *J. Comput. Phys*., *55*, 203-230.

[22] Twizell, E. H., Bratsos, A. G. & Newby, J. C. (1997). A finite-difference method for solving the cubic Schrödinger equation. *Math. Comput. Simul*., *43*, 67-75.

[23] Wu, L. (1996). DuFort-Frankel-type methods for linear and nonlinear Schrödinger equations. *SIAM J. Numer. Anal*., *33*, 1526-1533.

[24] Zhang, L. (2005). A high accurate and conservative finite difference scheme for nonlinear Schrödinger equation. *Acta Math. Appl. Sin*., *28*, 178-186.
[25] Xie, S. S., Li, G. X. & Yi, S. (2009). Compact finite difference schemes with high accuracy for one-dimensional nonlinear Schrödinger equation. *Comput. Methods Appl. Mech. Engrg*., *198*, 1052-1060.
[26] Herbst, B. M., Morris, J. L. & Mitchell A. R. (1985). Numerical experience with the nonlinear Schrödinger equation. *J. Comput. Phys*., *60*, 282-305.
[27] Tourigny, Y. & Morris, J. L. L. (1988). An investigation into the effect of product approximation in the numerical solution of the cubic nonlinear Schrödinger equation, *J. Comput. Phys*., *76*, 103-130.
[28] Dág, I. (1999). A quadratic B-spline finite element method for solving nonlinear Schrödinger equation. Comput. *Methods Appl. Mech. Eng*., *174*, 247-258.
[29] Karakashian, O. & Makridakis, C. (1998). A space-time finite element method for the nonlinear Schrödinger equation: the discontinuous Galerkin method. *Math. Comput*., *67*, 479-499.
[30] Xu, Y. & Shu, C. W. (2005). Local discontinuous Galerkin methods for nonlinear Schrödinger equations. *J. Comput. Phys*., *205*, 72-97.
[31] Korkmaz, A. & Dág, I. (2008). A differential quadrature algorithm for simulations of nonlinear Schrödinger equation. *Comput. Math. Appl*., *56*, 2222-2234.
[32] Korkmaz, A. & Dág, I. (2009). A differential quadrature algorithm for nonlinear Schrödinger equation. *Nonlinear Dyn*., *56*, 69-83.
[33] Dereli, Y., Irk, D. & Dág, I. (2009). Soliton Solutions for NLS Equation Using Radial Basis Functions. *Chaos Soliton Fract*., *42*, 1227-1233.
[34] Pathria, D. & Morris, J. L. L. (1990). Pseudo-spectral solution of nonlinear Schrödinger equations. *J. Comput. Phys*., *87*, 108-125.
[35] Sulem, P. L., Sulem, C. & Patera, A. (1984). Numerical simulation of singular solutions to the two-dimensional cubic Schrödinger equation. *Comm. Pure Appl., Math*., *37*, 755-778.
[36] Hu, X. G., Ho, T. S. & Rabitz, H. (2000). Solving the bound-state Schrödinger equation by reproducing kernel interpolation. *Phys. Rev*., *E61*, 59-67.
[37] Dereli, Y. (2012). The meshless kernel-based method of lines for the numerical solution of the nonlinear Schrödinger equation. *Eng. Anal. Bound. Elem*., *36*, 1416-1423.
[38] Aronszajn, N. (1950). Theory of reproducing kernels. *Trans. Amer. Math. Soc*., *68*, 337-404.
[39] Mokhtari, R., Toutian Isfahani, F. & Mohammadi, M. (2012). Reproducing kernel method for solving nonlinear differential-difference equations. *Abs. Appl. Anal*., Article ID 514103.
[40] Mohammadi, M. & Mokhtari, R. (2011). Solving the generalized regularized long wave equation on the basis of a reproducing kernel space. *J. Comput. Appl. Math*., *235*, 4003-4011.
[41] Geng, F. & Li, X. M. (2012). A new method for Riccati differential equations based on reproducing kernel and quasilinearization methods. *Abs. Appl. Anal*., Article ID 603748.
[42] Geng, F. & Cui, M. (2007). Solving a nonlinear system of second order boundary value problems. *J. Math. Anal. Appl*., *327*, 1167-1181.
[43] Yingzhen, L. & Yongfang, Z. (2009). Solving nonlinear pseudoparabolic equations with nonlocal boundary conditions in reproducing kernel space. *Numer Algor*., *52*, 173-186.
[44] Ablowitz, M. J., Prinari, B. & Trubatch, A. D. Discrete and continuous nonlinear Schrödinger systems. *Bull. Am. Math. Soc*., *43*, 127-132.
[45] Sanz-Serna, J. M. & Verwer, J. G. (1986). Conservative and nonconservative schemes for the solution of the nonlinear Schrödinger equation. *IMA J. Numer. Anal*., *6*, 25-42.
[46] Zakharov, V. E. & Shabat, A. B. (1972). Exact theory of two-dimensional self-focusing and one-dimensional self-modulation of waves in nonlinear media. *Soviet Phys. JETP*., *34*, 62-69.

Appendix

For constructing reproducing kernel function $R_y(x)$ in $W_0[a,b]$, according to (3) we have

$$\begin{aligned}\langle u(x), R_y(x)\rangle_{W_0} &= u(a)v(a) + u'(a)v'(a) + u(b)v(b) \\ &\quad + \int_a^b u^{(3)}(x)R_y^{(3)}(x)dx \\ &= u'(a)\left(R_{y\prime}(a) + R_y^{(4)}(a)\right) + u''(b)R_y^{(3)}(b) \\ &\quad - u''(a)R_y^{(3)}(a) \\ -u''(b)R_y^{(4)}(b) - \int_a^b u(x)R_y^{(6)}(x)dx. \end{aligned} \quad (8)$$

Since $R_y(x) \in W_0[a,b]$, it follows that

$$R_y(a) = 0, \quad R_y(b) = 0.$$

If

$$R_{y\prime}(a) + R_y^{(4)}(a) = 0, \quad R_y^{(3)}(a) = 0, \quad R_y^{(3)}(b) = 0, \quad R_y^{(4)}(b) = 0,$$

then (8) implies that

$$\langle u(x), R_y(x)\rangle_{W_0} = -\int_a^b u(x)R_y^{(6)}(x)dx.$$

For every x in $[a,b]$, if $R_y(x)$ also satisfies

$$R_y^{(6)}(x) = -\delta(x-y),$$

then

$$\langle u(x), R_y(x)\rangle_{W_0} = u(y).$$

Thus we introduce the analytical representation of $R_y(x)$. Consider the following boundary value problem with y as a parameter:

$$\begin{cases} R_y^{(6)}(x) = 0, \quad x \neq y; \\ R_y(a) = 0, \\ R_y(b) = 0, \\ R_{y\prime}(a) + R_y^{(4)}(a) = 0, \\ R_y^{(3)}(a) = 0, \\ R_y^{(3)}(b) = 0, \\ R_y^{(4)}(b) = 0, \\ R_y^{(k)}(x)|_{x=y^{-0}} = R_y^{(k)}(x)|_{x=y^{+0}}, \quad k = 0,1,2,3,4 \\ R_y^{(5)}(x)|_{x=y^{+0}} - R_y^{(5)}(x)|_{x=y^{-0}} = -1. \end{cases} \tag{9}$$

It can be shown that the solution of problem (9) is

$$R_y(x) = \begin{cases} c_1 + c_2 x + c_3 x^2 + c_4 x^3 + c_5 x^4 + c_6 x^5, & x \leq y \\ d_1 + d_2 x + d_3 x^2 + d_4 x^3 + \mathrm{d}_5 x^4 + d_6 x^5, & x > y \end{cases}$$

where the unknown coefficients can be obtained by applying the boundary conditions of (9).